Available online at www.eccomasproceedia.org
Eccomas Proceedia COMPDYN (2019) 5566-5578

ECCOMAS
Proceedia

COMPDYN 2019
7th ECCOMAS Thematic Conference on
Computational Methods in Structural Dynamics and Earthquake Engineering
M. Papadrakakis, M. Fragiadakis (eds.)
Crete, Greece, 24–26 June 2019

BASIN EDGE EFFECT AT TURKISH BASINS: THE CASE STUDY OF DINAR AND DUZCE BASINS

H. Khanbabazadeh[1], R. Iyisan[2], M.E. Hasal[3] and C. Zulfikar[4]

[1, 4] Assistant Professor, Gebze Technical University
Civil Eng. Department, 41400 Gebze, Kocaeli, Turkey
e-mail: hadikhanbabazadeh@gmail.com

[2] Professor, Istanbul Technical University
Civil Engineering Faculty, 34469 Maslak, Istanbul, Turkey
iyisan@itu.edu.tr

[3] Project Director, Bursa Metropolitan Municipality
Department of Construction, Bursa, Turkey
hasal@hotmail.com

[4] Assistant Professor, Gebze Technical University
Civil Eng. Department, 41400 Gebze, Kocaeli, Turkey
aczulfikar@gtu.edu.tr

Abstract

Several studies have revealed that the inclined bedrock at the sides of the basins bring about the concentration of damages, which well known as basin edge effect. As a seismically active area much of the Turkey lies on the Anatolian Plate. This small plate bounded by two major strike-slip fault zones, the North Anatolian Fault and East Anatolian Fault. During the history, Turkey has been the site of devastating earthquakes.

Severe structural damage at basin sides during recent major earthquakes around the world strongly pointed out the importance of basin edge effect. Some of its notable examples can be tracked in Turkey. With respect to the fact that Turkey is among the top 20 percent of all countries exposed to earthquake hazard with regard to mortality and economic losses, the necessity of the investigation and consideration of the basin edge effect in earthquake design codes is revealed. In this study, the dynamic behavior at the edge of two real basins is investigated. In this study, at the first, the basin edge model of the basins are extracted from the data obtained from extensive microtremor surveys and geotechnical investigations as well as in-situ studies including SPT, CPT, PS logging tests. Then, the idealized geometry of the Dinar and Duzce basins edge models are proposed.

Afterwards, the basins are subjected to the collection of strong ground motions using a fully nonlinear method which works based on explicit finite difference scheme FLAC3D code. The

ISSN:2623-3347 © 2019 The Authors. Published by Eccomas Proceedia.
Peer-review under responsibility of the organizing committee of COMPDYN 2019.
doi: 10.7712/120119.7327.19572

idealized 2D model of the Dinar and Duzce basins are subjected to the collection of sixteen strong ground motions with different peak ground accelerations (PGA) level of 0.1, 0.2, 0.3 and 0.4 g, four motions for each PGA level. For missing the effect of soil layers on selected real accelerograms they have been chosen from among those recorded on stiff layers during real earthquakes, or deconvoluted to the corresponding bedrock motion.

After the application of the strong ground motions from the bottom of the models in time domain, the acceleration of the surface points were recorded. For each surface point, the maximum spectral amplification factor under each earthquake is calculated then the average of resulted spectral amplification for four earthquakes of the same PGA level was estimated and reported.

The results of the dynamic analysis of Duzce basin showed the dominant effect of the inclined bedrock at the basin edge. Also, variation of its effect under excitations with different PGA levels is evident. At this basin the highest amplification factor occurs under the motions with PGA of 0.2g. Also, unlike the rest of the curves, a de-amplification of 0.85 along about 200 meters from the basin edge occurred at Duzce basin edge which shows that the basin edge can sometimes have decreasing effect on amplification. Regarding the influenced distance by the basin edge, while this distance is bout 800m and 1000m for the motions with the PGA of 0.1g and 0.2g, it increases to 1250m and 1500m for the motions with the PGA of 0.3g and 0.4g, respectively.

For asymmetric Dinar basin, two different amplification behaviors were seen at the eastern and western edges of the basin in terms of amplification amount and influenced distance by the basin edge. The higher basin edge effect at the eastern part with lower bedrock inclination with respect to western part was seen. This shows the higher effect of bedrock with lower angles. While the highest amplification factor at the western side occurs under the motions with PGA of 0.3g, it happens under the motions with PGA of 0.1g at the eastern side. Also, it was seen that at the eastern part of the basin has affected the distance about 1500 m from the outcrop while this distance for the steeper bedrock angle at the western side is about 700 m from outcrop. Between these distances 1D behavior is dominant.

The results show that the dynamic behavior of the both Dinar and Duzce basins at their sides is under the effect of basin edge in terms of amplification amount and influenced distance by the basin edge. At the basin edges, comparable amplification amounts with respect to the inner parts of the basins were seen.

Keywords: Site effect, Dynamic behavior, Numerical modeling, Microtremor, Basin edge effect, Dinar Basin, Duzce Basin.

1 INTRODUCTION

Several studies have revealed that the inclined bedrock at the sides of the basins bring about the concentration of damages, which well known as basin edge effect [1-3]. Ashigara Valley [4] and Ohba Valley [5] in Japan, Parkway Valley in New Zealand [6], Coachella Valley in southern California [7], Volvi Basin in Greece [8], Heathcote Valley in the Christchurch City of New Zealand [9] are among the sites with extensive seismic array observation instruments that have been used for validation of the theoretical studies regarding basin effects. In the meantime, investigations carried out at basins like Miyagi and Fukushima (Japan) [10], Fraser Delta [11] and Euroseistest site [12], among others, provided more accurate data about the basin edge effect.

As a seismically active area much of the Turkey lies on the Anatolian Plate. This small plate bounded by two major strike-slip fault zones, the North Anatolian Fault and East Anatolian Fault. During the history, Turkey has been the site of devastating earthquakes. A devastating earthquake hit the city of Duzce on November 12, 1999 with a moment magnitude (Mw) of 7.2 causing heavy damage and fatalities in Duzce province. The seen damage pattern during 1st October 1995 earthquake at Dinar town, Turkey, where located at the edge of an alluvial basin is another example of such effect. With respect to the statistical investigations, the resulting losses place Turkey in the top 20 percent of all countries exposed to earthquake hazard with regard to mortality and economic losses [13]. Severe structural damage at basin sides during recent major earthquakes around the world strongly pointed out the importance of basin edge effect and land-use planning [14-15]. Some of its notable examples can be tracked in Turkey. The recorded damage patterns during 1996 Dinar earthquake [16] as well as November 12, 1999 Duzce earthquake [17] revealed the necessity of the consideration of the basin edge effect in earthquake design codes. In this study, the different dynamic behavior at the edge of two basins with respect to the basin center is investigated. The results of such investigations can be used as the critical data in land-use planning projects as instrument of earthquake hazard mitigation.

In this study, at the first, the edge models of are extracted from the data obtained from performed microtremor surveys as well as geotechnical investigation. In this way, the basin stratification and shear wave velocity profile as well as geotechnical properties of the layers are obtained. Based on these data, the idealized geometry of Dinar and Duzce basins are proposed. Then, in order to estimate the dynamic behavior of the basins, a fully nonlinear method based on explicit finite difference scheme which solve the full equations of motion using FLAC3D code [18] is performed.

2 BASIN EDGE EFFECTS AT DINAR AND DUZCE BASINS

The existence of the inclined bedrock underlying the Duzce Basin has aroused the ideas of the effect of the basin edge on the dynamic behavior of basin. Also, the concentration of the damages at the edges of the non-symmetric alluvial Dinar basin indicates the involvement of the inclined bedrock in the different dynamic behavior of the basin at its sides [19-20].

2.1 Geology and seismo-tectonics of the basins

Dinar town is located at the edge of an alluvial basin in the southwest Anatolia, Turkey. To reveal its geology and geotechnical conditions, extensive in-situ studies including SPT, CPT, PS logging tests as well as microtremor measurements were carried out throughout the town [21].

There are two main fault systems around Dinar Town. One of them is Dinar-Civril fault which lays in the NW-SE direction and the other is Akdag fault with N-S direction. The Di-

nar-Civril fault has got a 75 km long normal fault with a slight oblique left lateral component [22]. These two fault systems had caused to form a seismotectonic structure consisting of two grabens and a horst.

In order to estimate the shear wave velocity profile of soil layers, at two of the pre-drilled boreholes suspension PS-logging tests until the approximate depths of 40 m were done. In Fig. 1 a characteristic geological section of Dinar laying in the E-W direction which reveals the horst-graben structure as well as an example of the results of the SPT and PS-logging test that were carried out at Dinar meteorological station site are presented.

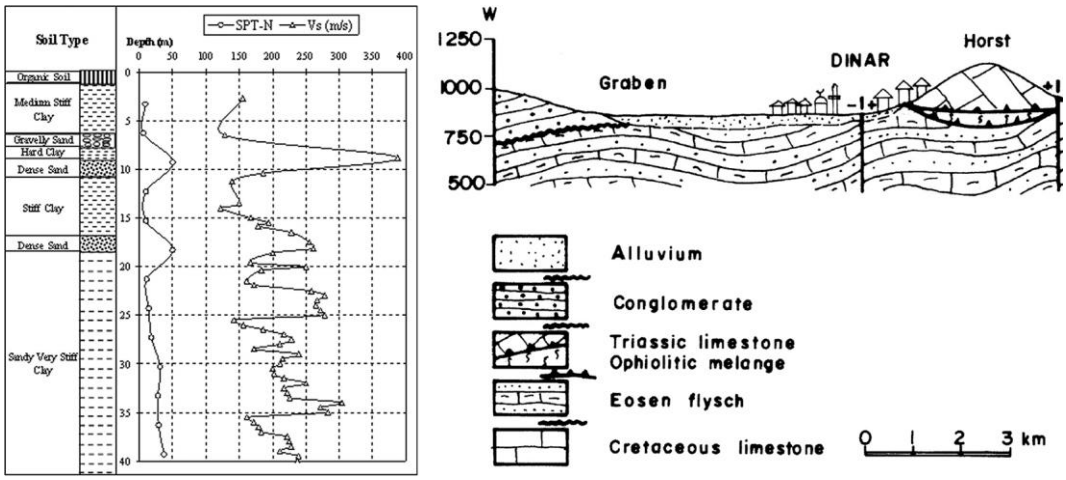

Figure 1: East-West geological section of Dinar basin and an example of the SPT and PS-logging test results.

Duzce basin is a graben-like basin which was formed by the activities of the North Anatolian Fault. From geological point of view there is a low inclined topography toward the southwest (toward Lake Eftani). In order to constitute the basin model and extract shear wave velocity profile of the Duzce basin a microtremor survey was performed. Also, Single point microtremor measurements were carried out at 25 different points in the basin along an S-N line. The thickness value for each top layer was estimated by providing the best fit between the H/V curve and theoretical Rayleigh wave ellipticity [23]. Based on microtremor measurements, the basin is composed of seven separate layers with different shear wave velocities. The layer with a shear wave velocity greater than 800 m/s was considered as seismic bedrock. The depth of seismic bedrock was estimated by the method conducted by Kudo et. al.(2002) [24]. In Fig. 2 the proposed Duzce basin stratification and the shear wave velocity profile of the basin edge is presented.

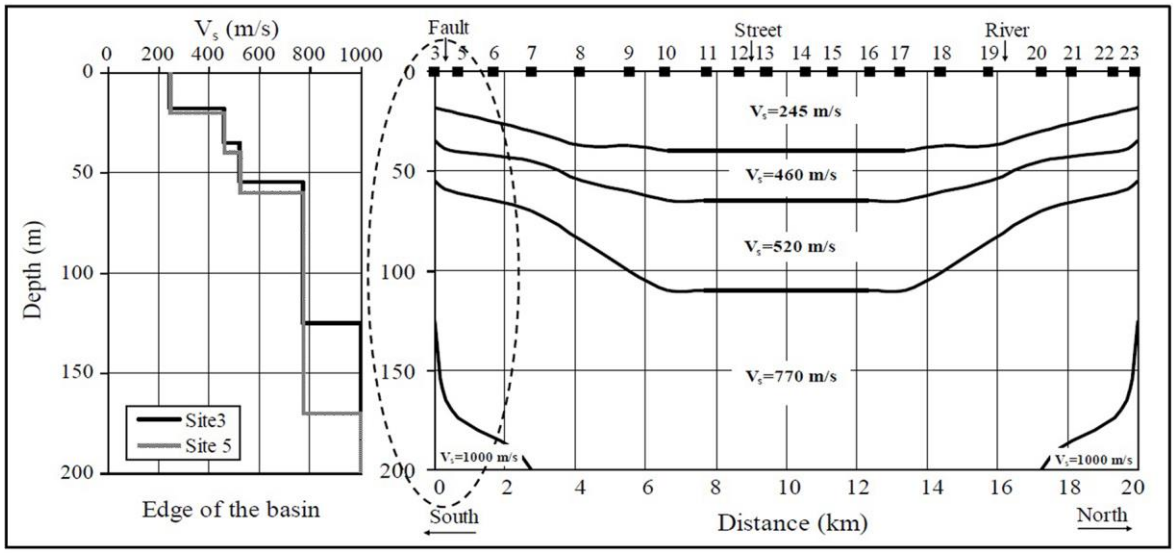

Figure 2: The proposed Duzce basin stratification and the shear wave velocity profile of the basin edge.

2.2 Idealized basin geometry and geotechnical properties

Based on the results of the microtremor measurements, underground explorations and laboratory tests, and with respect to the extracted geologic cross sections of the areas given at Fig. 1 and Fig.2 the idealized geometry of the Dinar and Duzce basins are proposed at Fig. 3.

As can be seen, for Dinar basin which is located between two horsts, the bedrock has got 6° inclination at the east edge until the180m depths. Then, until the depth of 220 m the bedrock angle decreases to 2°. At the west part steeper bedrock with 20° angle continues until the depth of 220 m. At the other parts, horizontal bedrock with the depth of 220 m is modeled. The width of the 2D basin model has been taken 6km.Corresponding soil specifications are presented at Table 1.

For Duzce basin, the findings of the 2D shear wave velocity profile indicate the seismic bedrock inclination of 6° at the basin edge which continues until 2km inside the basin. The soil layers were assumed to extend horizontally within 2.2 km from the basin edge. Also, in order to effectively catch the 2D behavior of the basin, the selected modeling length should exceed the region that is affected by inclined bedrock. Such point is considered as the beginning of the 1D behavior of the basin; the region that the effect of the inclined bedrock is missed. So, the left 2.2km of the basin has been modeled.

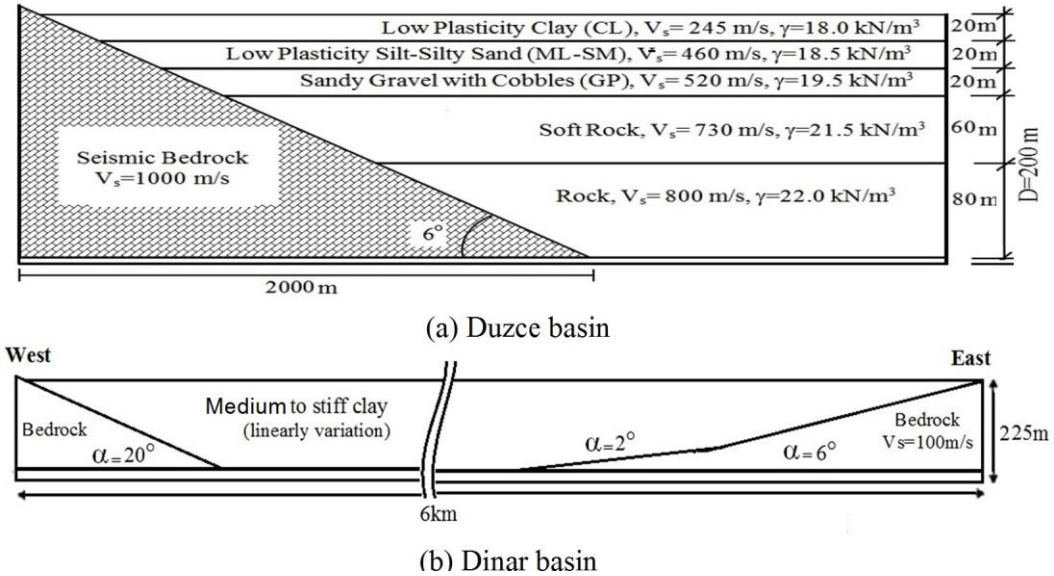

Figure 3: The idealized geometry of the (a) Duzce and (b) Dinar basins.

Regarding geotechnical properties of the basins, the 220 m basin depth of the Dinar basin is divided to two 200 m and 20 m layers on the bedrock in order to model the 20 m transient layer between bedrock and basin (underlying a 5m bedrock layer). A linear variation of the properties over basin depth has been provided for Dinar basin. Duzce basin and its surrounding area consists of alluvium deposits and lake sediments, which are composed of fine grained gravel, sand and silt mixture with clay layers. The geotechnical properties of the idealized Dinar and Duzce basins soils are presented at Table 1.

Soil Type	c' (kPa)	ϕ' (°)	Vs (m/s)	G (MPa)	K (MPa)	g(kN/m$^{3)}$
Dinar Basin						
Basin	50-140	10	175-600	55.1-828	143.7-2159	18-21.6
Transient part	140-150	10	600-700	828-1127	2159-2939	216-22
Bedrock	-	-	1000	2200	3600	22
Duzce Basin						
Stiff Low Plasticity Clay with Sand (CL)	10	26	245	108	282	18
Medium Dense-Dense Silty Sand (SM)	3	33	460	391.5	1020	18.5
Dense-Very Dense Sandy Gravel with Cobbles (GP)	-	38	520	527.3	1375	19.5
Medium Weathered Soft Rock	350	35	730	1120	2918	21
Slightly Weathered Soft Rock	450	37	800	1410	3672	22
Elastic Bedrock	-	-	1000	2500	4160	25

Table 1: The geotechnical properties of the idealized Dinar and Duzce basins

The idealized 2D model of the Dinar and Duzce basins are subjected to the collection of sixteen strong ground motions with different peak ground accelerations (PGA) level of 0.1, 0.2, 0.3 and 0.4 g, four motions for each PGA level. These records are of different peak ground accelerations, frequency contents and durations. They are baseline corrected and filtered by a 25 Hz low-pass filter. The excitations are applied as SV waves to the model bot-

toms. For missing the effect of soil layers on selected real accelerograms they have been chosen from among those recorded on stiff layers during real earthquakes, or deconvoluted to the corresponding bedrock motion. At Table 2 the specification of the applied earthquakes are presented.

Earthquakes	Station	Amax (g)	Magnitude	Significant Duration (s)	Arias Intensity (m/s)
Anza (25.02.1980)	PinyonFlat	0.1	Mw=4.9	1.945	0.0218
Mammoth lakes (25.05.1980)	LongValleyDam	0.1	Mw=6.0	7.46	0.0666
Chalfant (21.07.1986)	LongValleyDam	0.1	Mw=6.2	10.24	0.0638
Palm springs1986	Silent Valley	0.1	ML=5.9	6.14	0.0658
Livermore (27.01.1980)	Morgan Terr Park	0.2	Mw=5.4	3.42	0.1877
Düzce (12.11.1999)	Lamont-531	0.2	Mw=7.1	10.57	0.5283
Dinar 1995	Dinar station	0.2	ML=5	14.95	0.8096
Sakarya (11.11.1999)	Develop. burea	0.2	Md=5.7	3.11	0.1397
Firuzabad 20.06.1994	Firuzabad-ZRT	0.3	Mw=5.9	7.14	0.687
Parkfield (28.06.1966)	Temblor pre	0.3	Mw=6.1	4.29	0.3615
Coyotelake (06.08.1979)	Coyote Lake Dam	0.3	Mw=5.7	3.68	0.4003
Mendocino 1992	EEL River valley	0.3	ML=6.5	4.82	0.8079
South Iceland (17.06.2000)	Thjorsarbru	0.4	Mw=6.5	4.29	1.6125
UmbriaMarche (10.16.1997)	Colfiorito	0.4	Mw=4.3	4.57	0.6902
Parkfield (28.06.1996)	Temblorpre	0.4	Mw=6.1	3.19	0.5537
Kocaeli1(7.08.1999)	Develop. burea	0.4	Md=7.4	9.74	1.5843

Table 2: The specification of the applied strong ground motion collection.

3 ANALYSIS METHOD

To estimate the dynamic behavior of the Dinar and Duzce basins a fully nonlinear analysis using FLAC3D code (Fast Lagrangian Analysis of Continua) based on explicit finite difference scheme which solves the full equations of motion is applied. In this method, both shear and compressional waves are propagated together in a single simulation, and the material responds to the combined effect of both components. This aspect gets more important in the 2D modeling of the basin edge where the waves are trapped at low angle bedrock inclinations. Also, the method follows any prescribed nonlinear constitutive relation and since the strain increments (not tensors) relate to the stress tensors, therefore plastic yielding is modeled appropriately [18]. With respect to the selected soil properties, the corresponding G/Gmax curves have been estimated based on relation proposed by Ishibashi and Zhang (1993) [25] and is presented at Fig. 5.

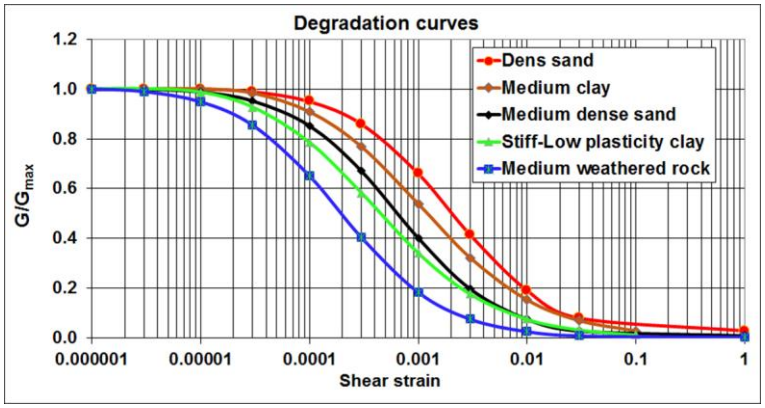

Figure 4: The corresponding G/Gmax degradation curves of the basins' soils.

At the bottom boundary of the model the quiet boundary scheme, which involves dashpots, are attached independently in the normal and shear directions to prevent the reflection of outward propagating waves back into the model as well as allow the necessary energy radiation. For vertical boundaries, the approach used in the continuum finite difference code NESSI [26] are developed via Free-Field boundary condition which involving the execution of free-field calculations in parallel with the main-grid analysis. Also, to provide the accurate transmission of the wave through modeled mesh, based on Kuhlemeyer and Lysmer (1973) [27], with respect to the frequency content of the input waves and the wave speed characteristics of the system, the spatial mesh size was selected smaller than one tenth to one eighth of the wavelength associated with the highest frequency component of the wave.

The verification of this analysis has been done by comparing to the solution of Kawase and Aki (1989) [28], and presented at Iyisan and Khanbabazadeh (2013) [29] and Khanbabazadeh and Iyisan (2014 a,b) [30-31]. The solution of the trapezoidal valley by Kawase and Aki (1989) [28] has been tested by Zahradnik (1995) [32] and Gil-Zepeda et al. (2003) [33], among the others.

4 RESULTS AND DISCUSSION

After the application of the strong ground motions presented at Table 2 from the bottom of the models in time domain, the acceleration of the surface points were recorded. For each surface point, the maximum spectral amplification factor under each earthquake is calculated then the average of resulted spectral amplification for four earthquakes of the same PGA level was estimated and reported. At Fig. 6 and Fig. 7, the maximum spectral amplification variation at the surface of the Dinar and Duzce basins under excitations with four different PGA levels are presented.

4.1 Dinar basin

As seen at the idealized geometry of the Dinar basin, this basin has got an asymmetric geometry with different bedrock angles at its sides. The effect of such geometry can also be seen in the dynamic behavior of Dinar basin at Fig. 6. Two different amplification behaviors are seen at the eastern and western edges of the Dinar basin in terms of amplification amount and influenced distance by the basin edge. Also, the effect of the motion strength on the dynamic behavior of the basin is evident.

The results show that while the highest amplification factor at the western side occurs under the motions with PGA of 0.3g (with the maximum amplification factor of 3.75), it hap-

pens under the motions with PGA of 0.1g at the eastern side (with the maximum amplification factor of 3.82).

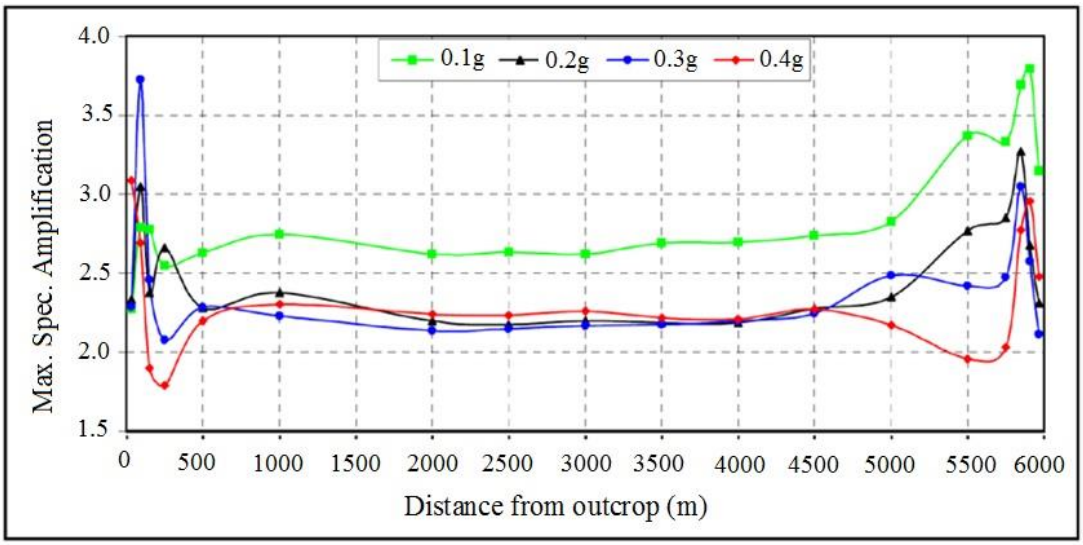

Figure 5: The maximum spectral amplification variation at Dinar basin surface.

There are two different amplification trends at two sides. Because of the enough distance between two edges, no interference of the edges effect is seen. In fact, Dinar basin is divided to three areas, two areas with independent 2D behavior at edges and a middle area with 1D behavior. The point that the amplification curve turns to a flat curve, which continues towards the inner parts of the basin, is usually considered as the beginning of the 1D behavior of the basin; the region that the effect of the inclined bedrock is missed.

It is seen that the milder bedrock inclination at the eastern part of the basin has affected the distance about 1500 m from the outcrop while this distance for the steeper bedrock angle at the western side is about 700 m from outcrop. Between these distances, the effects of the basin edges are cancelled. In this region the basin turns to behave one dimensionally. The highest 1D amplification factor belongs to the motions with PGA of 0.1g. For other PGA levels, relatively close 1D amplification factor is seen. While the sustained spectral amplification of the basin center under the motions of 0.1g PGA is about 2.7, it decreases to about 2.25 for stronger motions with higher PGAs.

4.2 Duzce basin

The amplification curves of the Duzce basin clearly show the influence of the basin edge on the dynamic behavior of Duzce basin. Also, the variation of its effect under excitations with different PGA levels is evident. As can be seen, while the highest amplification factor occurs under the motions with PGA of 0.2g, the lowest amplification factor belongs to the motions with PGA of 0.1g.

Despite the increasing trend of the amplification under the motions with the PGA of 0.1g and 0.2g, it begins to decrease under the motions with higher PGAs. The seen amplification factors under the motions with the PGA of 0.3g and 0.4g reach to 3.4 and 3, respectively.

Also, the maximum amplification curve of the basin surface under the motions with the PGA of 0.3g shows a de-amplification of 0.85 along about 200 meters from the basin edge, unlike the rest of the curves. This shows that the basin edge can sometimes have decreasing effect on amplification. This phenomenon can be the result of the trapping of the waves at the half space between inclined bedrock and surface at the edges.

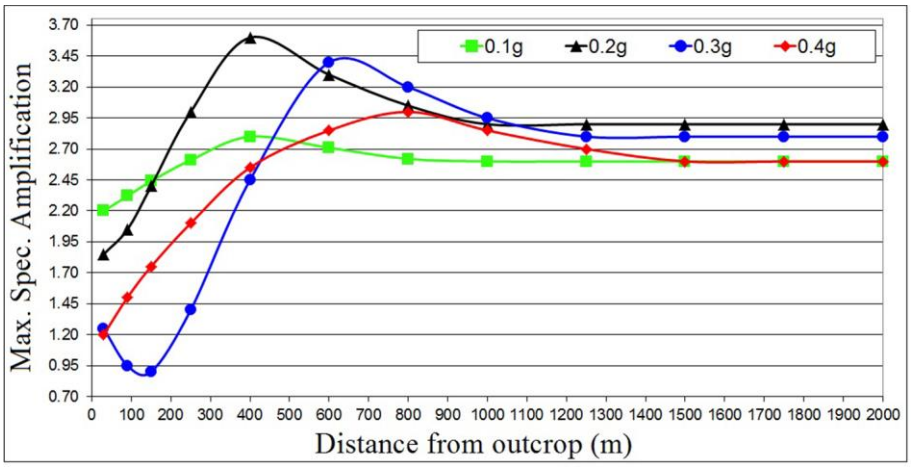

Figure 6: The maximum spectral amplification variation at Duzce basin surface.

As mentioned earlier, from the point that the effect of the inclined bedrock is missed the 1D behavior of the basin begins. For Duzce basin the beginning of 1D behavior under the motions with different strengths is different. While this behavior for motion with the PGA of 0.1g begins at 800m from the outcrop (with the maximum amplification factor of 2.6), it reaches to about 1000m under the motions with the PGA of 0.2g (with the maximum amplification factor of 2.9). Despite the decrease in the maximum amplification factor under the motions with the PGA of 0.3g and 0.4g (with respect to the motions with the PGA of 0.2g), the beginning point of the 1D behavior stretches more. It begins from 1250m and 1500 for the motions with the PGA of 0.3g and 0.4g, respectively. In shorts, inside these areas the effect of the basin edge is dominant.

5 CONCLUSIONS

- In this study, in order to investigate the basin edge effect, at the first, the basin edge model is extracted from the data obtained from extensive microtremor surveys and geotechnical investigations as well as in-situ studies including SPT, CPT, PS logging tests. Using these findings the basin stratification and shear wave velocity profile as well as geotechnical properties of the layers of the basins were obtained. Then, the idealized geometry of the Dinar and Duzce basins edge models were proposed. Afterwards, the basins were subjected to the collection of sixteen strong ground motions with different peak ground accelerations (PGA) levels using a fully nonlinear method which works based on explicit finite difference scheme and solve the full equations of motion using FLAC3D code. Using the recorded acceleration at 12 surface points along the basin edge the variation of the maximum spectral amplification factor was reported.

- The results show that the dynamic behavior of the both Dinar and Duzce basins at their sides is under the effect of basin edge. Comparable amplification amounts with respect to the inner parts of the basins were seen. For asymmetric Dinar basin, two different amplification behaviors were seen at the eastern and western edges of the basin in terms of amplification amount and influenced distance by the basin edge. The higher basin edge effect at the eastern part with lower bedrock inclination with respect to western part was seen. This shows the higher effect of bedrock with lower angles. While the highest amplification factor at the western side occurs under the motions with PGA of 0.3g, it happens under the motions with PGA of 0.1g at the eastern side. Also, it was seen

that at the eastern part of the basin has affected the distance about 1500 m from the outcrop while this distance for the steeper bedrock angle at the western side is about 700 m from outcrop. Between these distances 1D behavior is dominant.

- The results of the dynamic analysis of Duzce basin showed the dominant effect of the inclined bedrock at the basin edge. Also, variation of its effect under excitations with different PGA levels is evident. At this basin the highest amplification factor occurs under the motions with PGA of 0.2g. Also, unlike the rest of the curves, a de-amplification of 0.85 along about 200 meters from the basin edge occurred at Duzce basin edge which shows that the basin edge can sometimes have decreasing effect on amplification. Regarding the influenced distance by the basin edge, while this distance is bout 800m and 1000m for the motions with the PGA of 0.1g and 0.2g, it increases to 1250m and 1500m for the motions with the PGA of 0.3g and 0.4g, respectively.

- By consideration of the all aspects of this study, the results of such investigations can be used as the critical data in land-use planning projects as instrument of earthquake hazard mitigation.

REFERENCES

[1] H. Khanbabazadeh, A. Janalizadeh, Investigation of the site effect on seismic ground motions using elasto-plastic constitutive model. *Elec. J. Geotech. Eng.,* 11(Bundle A), 2006.

[2] D. Assimaki, S. Jeong, Coupled topography-stratigraphy effects during the m 7.0 Haiti earthquake: the case of hotel Montana. *4th IASPEI/IAEE international symposium,* Santa Barbara: University of California, USA, 2011.

[3] M. E.Hasal, R. Iyisan, H. Khanbabazadeh, A. Bayin, G. Cevikbilen, O. Kepceoglu. A, Preliminary Seismic Microzonation Study Based on Microtremor Measurements. *International Conference on Earthquake Engineering*, Skopje, Macedonia, 2013.

[4] A. Ohtsuki, H. Yamahara, T. Tazoh, Effect of lateral inhomogeneity on seismic waves, II: Observation and analysis. *Earthq Eng Struct Dyn.,* **12**:795-816, 1984.

[5] G. Gazetas, K. Fan, T. Tazoh, K. Shimizu. Seismic response of the pile foundation of Ohba Ohashi Bridge. *Proceedings of the 3rd International Conference on Case History in Geotechnical Engineering*, 1803-1809, 1993.

[6] F.J. Chavez-Garcia, M. Rodriguez, W.R. Stephenson. 1D vs. 2D site effects: the case of Parkway Basin, New Zealand. *11th European Conference on Earthquake Engineering,* Balkema, Rotterdam, 1998.

[7] E.H. Field, Spectral amplification in a sediment-filled valley exhibiting clear basin edge induced waves. *Bull Seismol Soc Am,* **86**, 991-1005, 1996.

[8] K. Pitilakis, Site effects. Recent Advances in Earthquake Geotechnical Engineering and Microzonation. *Kluwer Academic Publishers*, Netherlands, 1:139-193, 2004.

[9] F. Gelagoti, R. Kourkoulis, D. Tsirantonaki, G. Gazetas, 2-dimensional non-linear valley effects at Heathcote Valley during the 2011 Canterbury earthquake: A case study. *2nd European Conference on Earthquake Engineering and Seismology*, Istanbul, 2014.

[10] M. Kamiyama, T. Satoh, Seismic response analysis of laterally inhomogeneous ground with emphasis on strains. *Soil Dyn Earthq Eng*, **22**, 877–84, 2002.

[11] W.D. Finn, E. Zhai, T. Thavaraj, X.S. Hao, C.E. Ventura, 1D and 2D analyses of weak motion data in Fraser Delta from 1966 Duvall earthquake. *Soil Dyn Earthq Eng*, **23**, 323–9, 2003.

[12] K. Makra, F.J. Chavez-Garcıa, D. Raptakis, K. Pitilakis, Parametric analysis of the seismic response of a 2D sedimentary valley: implications for code implementations of complex site effects. *Soil Dyn Earthq Eng*, 25, 303–15, 2005.

[13] M. Erdik, Earthquake Risk in Turkey. *Am Assoc Advanc Sci*, **341(6147)**,724-725, 2013. DOI: 10.1126/science.1238945.

[14] K. Beyen, M. Erdik, Two-dimensional nonlinear site response analysis of Adapazarı plain and predictions inferred from aftershocks of the Kocaeli earthquake of 17 August 1999. *Soil Dyn Earthq Eng*, **24**, 261-279, 2004. DOI:10.1016/j.soildyn.2003.10.009.

[15] H. Khanbabazadeh, R. Iyisan, A. Ansal, C. Zulfikar, Nonlinear dynamic behavior of the basins with 2D bedrock. *Soil Dyn Earthq Eng*, **107**,108-115, 2018;. DOI: 10.1016/j.soildyn.2018.01.011.

[16] KOERI. Dinar earthquake of 1.10. Reconnaissance Report, October 9, 1995. Bogazici University, Kandilli Observatory and Earthquake research Institute (KOERI); 1995.

[17] M.E. Hasal, R. Iyisan, H. Yamanaka, Basin Edge Effect on Seismic Ground Response: A Parametric Study for Duzce Basin Case, Turkey. *Arab J Sci Eng*, **43(4)**, 2069–2081, 2018.

[18] P.A. Cundall. FLAC3D Manual: A Computer Program for Fast Lagrangian Analysis of Continua (Version 4.0), Minneapolis, Minnesota, USA; 2008.

[19] B.S. Bakir, M.Y. Ozkan, S. Ciliz, Effects of basin edge on the distribution of damage in 1995 Dinar, Turkey earthquake. *Soil Dyn Earthq Eng*, **22**, 335–45, 2002.

[20] H. Khanbabazadeh, R. Iyisan. A. Ansal, M.E. Hasal, 2D non-linear seismic response of the Dinar basin,TURKEY. *Soil Dyn Earthq Eng*, **89:5**–11, 2016.

[21] M.A. Ansal, R. Iyisan, H. Güllü, Microtremor measurements for the microzonation of Dinar. Pure Appl Geophys, **158**, 2525–41, 2001.

[22] A. Ozturk, Tectonics of Dinar Sandıklı-Isıklı region, Communications of Faculty of Science. Ankara, Turkey: University of Ankara; .pp 1–58, 1982.

[23] H. Yamanaka, M. Kato, M. Hashimoto, U. Gulerce, R. Iyisan, A. Ansal, Microtremor and earthquake observations in Adapazari and Duzce, Turkey, for estimations of site amplifications. *Proceedings of the Assessment of Seismic Local Site Effects at Plural Test Sites, Ministry of Education, Science, Sports and Culture, Research Grant No: 11694134*, Japan, 129-136, 2002.

[24] K. Kudo, T. Kanno, H. Okada, O. Ozel, M. Erdik, T. Sasatani, S. Higashi, M. Takahashi, K. Yoshida, Site-specific issues for strong ground motions during the Kocaeli, Turkey, earthquake of 17 August 1999, as inferred from array observations of microtremors and aftershocks. *Bulletin of Seismological Society of America,* **92 (1),** 448-465, 2002.

[25] I. Ishibashi, X. Zhang, Unified dynamic shear moduli and damping ratios of sand and clay. *Soils Found Jpn Soc Soil Mech Found Eng*, **33(1),** 182–91, 1993;.

[26] P.A. Cundall. et al., NESSI–Soil Structure Interaction Program for Dynamic and Static Problems, *Norwegian Geotech. Institute; Report*, **51**,508-509, 1980.

[27] R.L. Kuhlemeyer, J. Lysmer, Finite element method accuracy for wave propagation problems. *J Soil Mech Found Div ASCE*, **99(SM5)**, 421–7, 1973.

[28] H. Kawase, K. Aki, A study on the response of a soft basin for incident. S, P and Rayleigh waves with special reference to the long duration observed in Mexico City. *Bull Seismol Soc Am*, **79**, 1361–82, 1989.

[29] R. Iyisan, H. Khanbabazadeh, A numerical study on the basin edge effect on soil amplification. *Bull Earthq Eng*, **11**, 1305–23, 2013.

[30] H. Khanbabazadeh, R. Iyisan, A numerical study on the 2D behavior of the single and layered clayey basins. *Bull Earthq Eng*, **12(4)**, 1515–36, 2014.

[31] H. Khanbabazadeh, R. Iyisan, A numerical study on the 2D behavior of the clayey basins. *Soil Dyn Earthq Eng*, **66**, 31-41, 2014. DOI:10.1016/j.soildyn.2014.06.029

[32] J. Zahradnik, Simple elastic finite-difference scheme. *Bull Seismol Soc Am*, **85**, 1879–87, 1995.

[33] S.A. Gil-Zepeda, J.C. Montalvo-Arrieta, R. Vai, F.J. Sanchez-Sesma, A hybrid indirect boundary element-discrete wave number method applied to simulate the seismic response of stratified alluvial valleys. *Soil Dyn Earthq Eng* , **23**, 77–862003.